

An Oceanic Impact of the Kuroshio on Surface Air Temperature on the Pacific Coast of Japan in Summer: Regional H₂O Greenhouse Gas Effect

HIROSHI G. TAKAHASHI

Tokyo Metropolitan University, Tokyo, and Japan Agency for Marine-Earth Science and Technology, Yokohama, Japan

SACHIHO A. ADACHI

Advanced Institute for Computational Science, RIKEN, Kobe, Japan

TOMONORI SATO

Faculty of Environmental Earth Science, Hokkaido University, Sapporo, Japan

MASAYUKI HARA

Center for Environmental Science in Saitama, Kazo, Saitama, Japan

XIEYAO MA AND FUJIO KIMURA

Japan Agency for Marine-Earth Science and Technology, Yokohama, Japan

(Manuscript received 8 November 2014, in final form 8 June 2015)

ABSTRACT

This study used a 4-km resolution regional climate model to examine the sensitivity of surface air temperature on the Pacific coast of Japan to sea surface temperature (SST) south of the Pacific coast of Japan during summer. The authors performed a control simulation (CTL) driven by reanalysis and observational SST datasets. A series of sensitivity experiments using climatological values from the CTL SST datasets over a 31-yr period was conducted. The interannual variation in surface air temperature over the Pacific coast was well simulated in CTL. The interannual variation in SST over the Kuroshio region amplified the interannual variation in surface air temperature over the Pacific coast. It was found that 30% of the total variance of interannual variation in surface air temperature can be controlled by interannual variation in SST. The calculated surface air temperature on the Pacific coast increased by 0.4 K per 1-K SST warming in the Kuroshio region. Note that this sensitivity was considerably greater during nighttime than during daytime. Concurrent with the warming in surface air temperature, downward longwave radiation at the surface was also increased. In summer, the increase in latent heat flux was considerably larger than that in sensible heat flux over the ocean because of SST warming, according to the temperature dependence of the Bowen ratio. This implies that the primary factor for the increase in surface air temperature in summer is increased moisture in the lower troposphere, indicating that the regional warming was caused by an increase in H₂O greenhouse gas.

1. Introduction

Recently, extremely hot weather has been observed occasionally over Japan. The frequency of extremely hot

weather probably increases because of the increase in mean temperature—namely, global warming—when natural variability is basically unchanging. The extreme hot weather poses health hazards to humans, particularly over the Pacific side of Honshu (the main island of Japan), Japan, which includes densely populated urban areas, such as Tokyo and Nagoya.

Extremely high temperatures on the Pacific side of Honshu are generally associated with the westward extension of the western Pacific subtropical high over the

 Denotes Open Access content.

Corresponding author address: Hiroshi G. Takahashi, Tokyo Metropolitan University, 1-1 Minami-Osawa, Hachioji, Tokyo 192-0397, Japan.
E-mail: hiroshi3@tmu.ac.jp

DOI: 10.1175/JCLI-D-14-00763.1

western North Pacific. Two primary explanations for the development of this system have been examined by many previous studies. One is the impact of tropical convection around the Philippine Sea, which has been referred to as the Pacific–Japan pattern (e.g., Nitta 1987). The detailed structure and mechanism of the Pacific–Japan pattern have been investigated (e.g., Kosaka and Nakamura 2006). The other explanation is the impact of midlatitude planetary wave activities (Enomoto et al. 2003).

However, one of the strongest warm western boundary currents in the world—namely, the Kuroshio—exists along the Pacific coast of Japan and can also control the regional climate over the Pacific side of Honshu. Warmed air masses over the higher sea surface temperature (SST) regions of the Kuroshio can be transported to the Pacific side of Honshu in the lower troposphere, because this island is located downstream of the southerly winds that flow along the periphery of the western Pacific subtropical high. These southerlies are climatologically predominant over the island in summer. Thus, the SST in the Kuroshio region, which is located over the coastal ocean south of Japan, can control the regional climate over the Pacific coast.

Previous studies have examined the significant impact of the SST of a warm western boundary current on the atmosphere. Minobe et al. (2008) showed that surface wind convergence enhanced evaporation and precipitation over the axis of the Gulf Stream current, and Minobe et al. (2010) investigated seasonal differences in the atmospheric response to the Gulf Stream. Koseki and Watanabe (2010) investigated the atmospheric response to SST anomalies on a scale of a few hundred kilometers over the Kuroshio Extension in winter, which could be clearly observed in the atmospheric boundary layer. Xu et al. (2010) examined the atmospheric impact of the 2004/05 Kuroshio large meander event and suggested that the cool water pool caused a reduction in surface wind speed and precipitation based on a 1-month experiment conducted in January 2005. These studies demonstrate the influence of SST on the atmosphere over and around western boundary currents.

However, long-term quantitative estimations of the influence of SST on the atmosphere are limited. To understand the statistically robust contribution of SST to the atmosphere, long-term or multiple-case experiments are required, because the atmospheric response to SST anomalies can vary under different atmospheric conditions (e.g., Peng et al. 1997). Additionally, long-term climate simulation permits us to investigate the extent to which the interannual variations in SST actually influence regional climate on interannual time scales. Moreover, we may demonstrate long-term changes in these influences.

It is also very difficult to isolate the impact of SST on the atmosphere from observation datasets because of

air–sea interactions. Generally, SST and surface air temperature are highly correlated (see section 3a). Specifically, the increase in surface air temperature over the Pacific side can be explained by advection of warmer air from the region of increased SST, which is referred to as an oceanic impact. However, a portion of the increase in surface air temperature could be the result of enhanced downward shortwave radiation at the surface caused by the extension of the western Pacific subtropical high; that is, an atmospheric impact. Therefore, the separation of oceanic and atmospheric impacts from data analysis of observational and reanalysis data is difficult.

At the local scale, the responses of air temperature in the lower troposphere to SST may alter the local circulation in coastal regions. In particular, changes in surface pressure over the warm SST should be adjusted (e.g., Lindzen and Nigam 1987). Additionally, the development of the planetary boundary layer due to the warm SST results in downward momentum transport (e.g., Wallace et al. 1989), which accelerates or decelerates wind speed in the planetary boundary layer.

This paper focuses on the oceanic impact on regional climate along the Pacific side. We quantitatively estimate the impact of SST in the Kuroshio region on the regional climate over the Pacific coast and focus on the interannual variation in regional climate. We attempt to determine the extent to which interannual variation in regional climate is controlled by the SST around Japan, particularly that of the western boundary current.

The remainder of this paper is organized as follows. Section 2 describes the data used in this study and the design of our numerical experiments. Section 3 presents the sensitivity of surface air temperature to interannual variation in SST. The contribution mechanism of sensitivity of surface air temperature to SST is discussed in section 4, and our conclusions are presented in section 5.

2. Numerical experiment and data

a. Model and experimental setup

To understand the impact of SST on surface air temperature over the Pacific side of Honshu, we conducted numerical experiments using a nonhydrostatic regional climate model, the Advanced Research Weather Research and Forecasting (ARW-WRF) Modeling system (hereafter ARW), version 3.4 (Skamarock et al. 2008). For initial and boundary conditions, we used the atmospheric conditions from the ERA-Interim product (Berrisford et al. 2009; <http://www.ecmwf.int/en/research/climate-reanalysis/era-interim>) of the European Centre for Medium-Range Weather Forecasts (ECMWF) and SST from the Optimum Interpolation Sea Surface Temperature, version 2 (OISST2; Reynolds et al. 2002;

<http://www.esrl.noaa.gov/psd/data/gridded/data.noaa.oisst.v2.html>). We refer to the experiments conducted in this study as the control (CTL). To investigate the impact of large-scale SST in a simple manner, we used monthly mean SST data. The monthly SST data were linearly interpolated with time, which was prescribed every 6 h. The Pacific side of Japan facing the western boundary current was selected as the computational target region. The model domains are shown in Fig. 1. We conducted 31 one-month time-slice control experiments in summer. We selected the month of August from 1982 to 2012 (i.e., 31 months) as the primary simulation period. The simulation period was defined as extending from 1 July to 1 September of each year. The first 31 days of each simulation were not used for analysis but as a spin-up period. This long spin-up period was necessary for the spinup of soil moisture. The horizontal grid increment of the coarse domain was 16 km, and that of the two-way nested domain was 4 km. Both domains had 27 terrain-following vertical levels. Moreover, because cumulus convective parameterization (CCP) controls not only convective systems but also the related atmospheric circulation through thermodynamic effects, sensitivity experiments may depend almost exclusively on CCP. Because test simulations with CCP showed an unrealistic amount of precipitation, we did not apply CCP in either domain. The Mellor–Yamada–Janjić planetary boundary layer scheme (Janjić 1994), the ARW single-moment six-class microphysics scheme (Hong and Lim 2006), the unified Noah land surface model (Chen and Dudhia 2001), and the Rapid Radiative Transfer Model for GCM applications (RRTMG) longwave and shortwave radiation schemes (Iacono et al. 2008) were used.

b. Sensitivity experiments

To understand the impact of SST, we conducted a series of sensitivity experiments: that is, 31 one-month experiments for August 1982–2012. The numerical design of these experiments was the same as that of CTL, except that SST over the whole domain was replaced by the climatology from 1982 to 2012. These sensitivity experiments are referred to as climatological SST (ClimSST). Figure 2 shows the August climatological SST distribution from 1982 to 2012. Higher SST, approximately 26°–28°C, is observed south of Japan. The interannual standard deviation is approximately 0.6–0.8 K.

Here, we discuss the limits of the experimental framework of this study. There are two main limitations. Air–sea interactions were not considered because we used an atmosphere-only model with prescribed SST. As a future study, the effect of air–sea interaction on interannual variations in regional climate should be estimated qualitatively and quantitatively. Second, the atmospheric lateral boundary conditions in both experiments are affected by

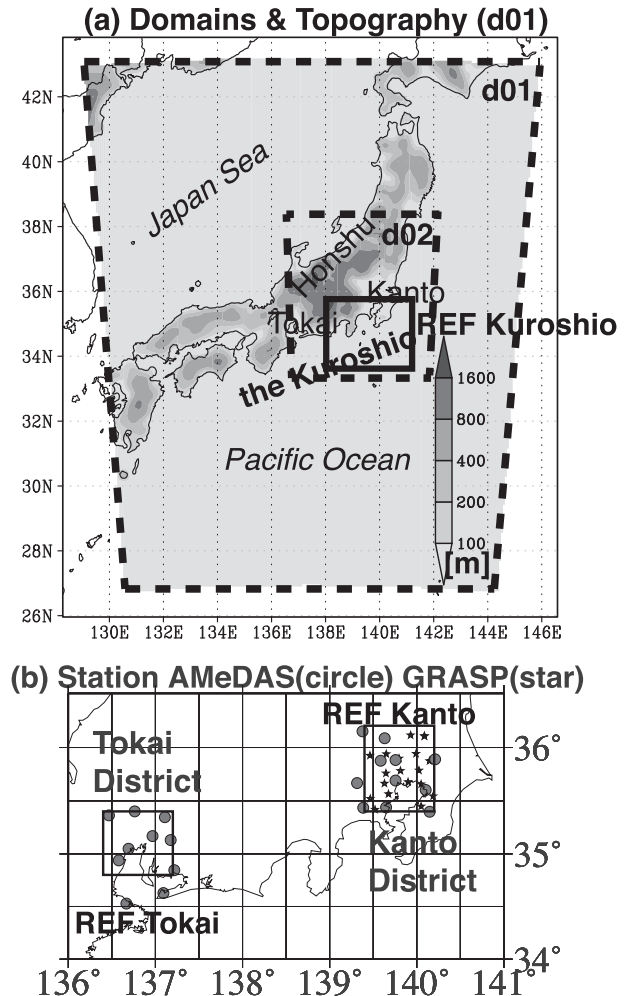


FIG. 1. (a) Study area, geographical names, and topography in domain 1. (b) Location of AMeDAS and GRASP–precipitable water stations and reference areas of the Kanto and Tokai Districts. The reference regions, REF Kuroshio (ocean at 33.5°–35.5°N, 138°–141°E) in (a), REF Kanto (land at 35.4°–36.2°N, 139.4°–140.2°E) in (b), and REF Tokai (land at 34.8°–35.4°N, 136.4°–137.2°E) in (b) are shown.

remote SST conditions, and we could not evaluate an SST impact at a scale larger than the outer calculation domain. Specifically, in both experiments, we prescribed the same Asian monsoon circulation, which had been affected by the SST condition over the Niño-3.4 region, as the atmospheric lateral boundary conditions. Thus, we only evaluated the impact of regional and local SST within the outer calculation domain on regional climate.

c. Observed data

We used surface air temperature data from the Automated Meteorological Data Acquisition System (AMeDAS; <http://www.jma.go.jp/jma/en/Activities/observations.html>) of the Japan Meteorological Agency. The monitoring stations used in this study are shown in

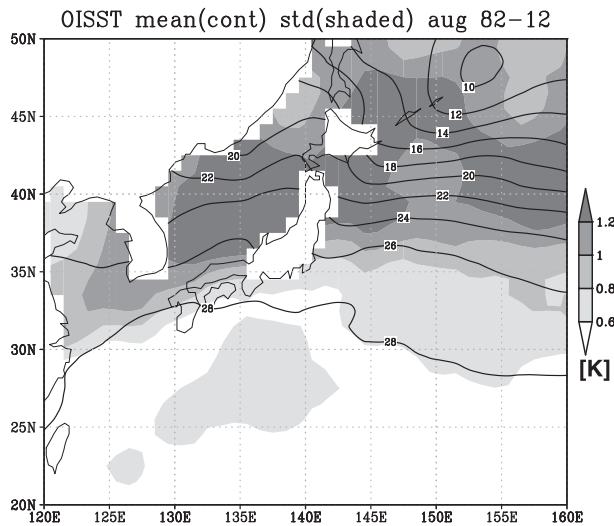


FIG. 2. Climatological mean SST (contours; °C) and its interannual standard deviation (shading; K) in August during the 31-yr period from 1982 to 2012.

Fig. 1b. We also used GPS Precipitable Water Research Project (GRASP) water vapor datasets (Fujita et al. 2012) derived from a global positioning system for the evaluation of simulated precipitable water. The observation datasets were averaged for the Kanto and Tokai Districts, respectively. The monitoring stations were selected with regard to spatial homogeneity. To confirm the low-level atmospheric circulation simulated in CTL, we used the Japanese 55-year Reanalysis Project (JRA-55; Kobayashi et al. 2015; http://jra.kishou.go.jp/JRA-55/index_en.html) dataset, including 950-hPa zonal and meridional winds (u , v), which is different from the driving atmospheric data, ERA-Interim.

d. Reference regions

To investigate the change in regional climate caused by changes in SST over the Kuroshio region, we refer to the Kuroshio reference region as (REF Kuroshio) (Fig. 1a). REF Kuroshio was selected to examine the impact of SST on the most densely populated urban area, Tokyo. Additional sensitivity experiments to investigate the oceanic impact of only REF Kuroshio are given in the appendix. Additionally, portions of the Kanto and Tokai Districts were taken as reference regions (REF Kanto and REF Tokai) to examine changes in the regional climates (Fig. 1b). Detailed locations are given in the caption of Fig. 1.

3. Results

a. Observed correlation between surface air temperature and SST

This subsection investigates the observed relationship between surface air temperature in the Kanto District

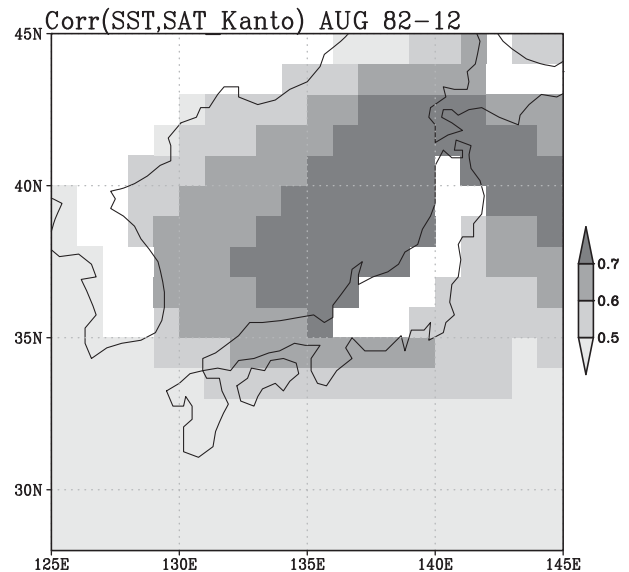


FIG. 3. Correlation coefficients between 11-point averaged observed surface air temperature in August over the Kanto District and SST during the 31-yr period from 1982 to 2012. The 11 monitoring stations are shown in Fig. 1b.

and SST on an interannual time scale. We calculated interannual correlation coefficients between monthly averages of observed surface air temperature at the 11 AMeDAS stations over the Kanto District and observed SST around Japan.

High correlations were found over the Sea of Japan and over the Japanese southern and eastern coastal regions of the western North Pacific (Fig. 3). These results suggest an SST effect over the Kuroshio, which is located over the southern coastal ocean. However, the physical explanation is complex. The extension of the western Pacific subtropical high over Japan induces enhanced downward shortwave radiation at the surface because the extension of the western Pacific subtropical high reduces cloud fractions over and around Japan. Thus, the ocean surface is simultaneously warmed by the increase in downward shortwave radiation at the surface.

Therefore, the high correlations may be partly explained as the impact of SST on surface air temperature, which can be referred to as an oceanic impact. However, a portion of the high correlations could be the result of the extension of the western Pacific subtropical high: that is, an atmospheric impact. To distinguish between atmospheric and oceanic impacts, we conducted two series of numerical experiments (CTL and ClimSST) with different oceanic boundary conditions.

b. Evaluation of CTL

To investigate the impact of SST on interannual variation in surface air temperature, we first evaluated the

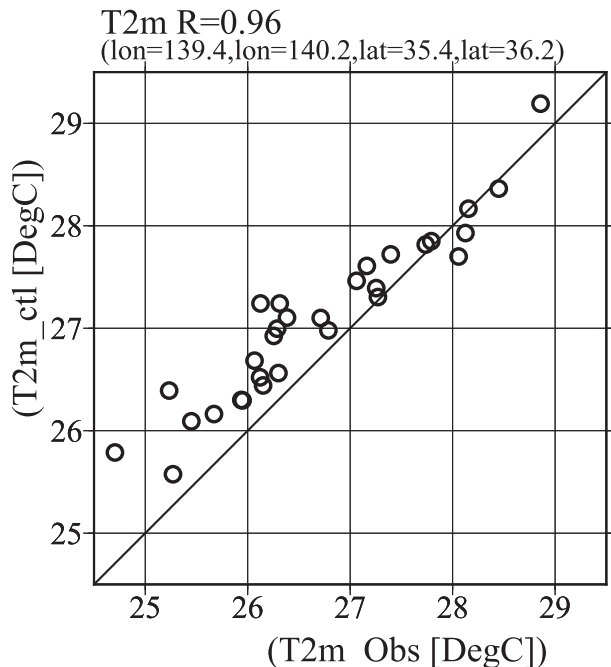


FIG. 4. Scatter diagram between the 11-point averaged observed monthly mean surface air temperature in August over the Kanto District and the area-averaged simulated monthly mean surface air temperature. Averaged surface air temperatures at 11 monitoring stations are shown (Fig. 1). The simulated surface air temperature is averaged over REF Kanto. The interannual correlation coefficient, bias, and root-mean-square error between the observed and simulated values during the 31-yr period from 1982 to 2012 were 0.96, +0.41, and 0.55, respectively.

performance of the interannual variation in the simulated regional climate over the Pacific side. Figure 4 shows a scatter diagram of monthly mean values of observed and simulated surface air temperature over REF Kanto (Fig. 1b). Observed monthly mean values for surface air temperature were derived from averaged values from 11 AMeDAS stations, and simulated values for surface air temperature were area averaged over REF Kanto.

The interannual variation in surface air temperature was well simulated with an interannual correlation coefficient of 0.96 (Fig. 4). The mean bias and root-mean-square error between the observed and simulated values were +0.41 and 0.55, respectively. Although warm biases were found in most years (Fig. 4), the simulated surface air temperature agreed with the observation, which indicates that the absolute values for surface air temperature were also well simulated. Additionally, we evaluated precipitation over REF Kanto. The correlation coefficient was 0.64, which indicates that interannual variation in precipitation was basically simulated (Fig. 5). However, precipitation was sometimes

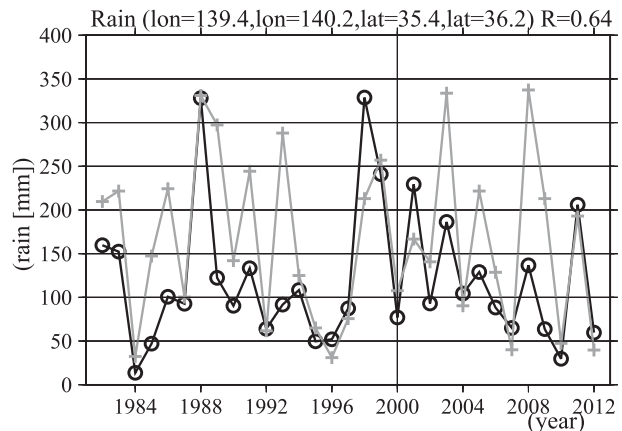


FIG. 5. Time series of the simulated precipitation in August over REF Kanto and the 11-point averaged observed precipitation (Fig. 1b). The heavy black line with the open circles refers to the simulated values of precipitation, and the gray line with plus signs is the observed precipitation. The interannual correlation coefficient, bias, and root-mean-square error between observed and simulated values were 0.64, −45.0, and 87.1, respectively, during the 31-yr period from 1982 to 2012.

underestimated, particularly in the high precipitation years. The mean bias and root-mean-square error of precipitation over REF Kanto between observed and simulated values were −45.0 and 87.1, respectively, during the 31 years from 1982 to 2012.

In section 4, we examine changes in precipitable water associated with downward longwave radiation at the surface to discuss the physical process of the variation of surface air temperature. Therefore, we here evaluate the simulated precipitable water. Available water vapor data were very limited particularly over land, although a microwave imager can estimate precipitable water over the ocean.

The interannual variation in precipitable water was well simulated in CTL (Fig. 6), with an interannual correlation coefficient of 0.94 during the 15 years from 1996 to 2010. Thus, the simulated interannual variation in precipitable water amount was sufficiently realistic to consider the effect of water vapor. Moreover, the mean bias and root-mean-square error of precipitable water over REF Kanto between observed and simulated values were +1.17 and 1.55, respectively, over the 15 years from 1996 to 2010, which indicates that the total amounts of precipitable water were also simulated very well.

Furthermore, we confirmed the low-level circulation over domain 2 (Fig. 7) by comparing with reanalysis data (JRA55; not shown), which differed from the driving atmospheric data for the simulations. Climatological low-level southerlies were simulated, showing that these

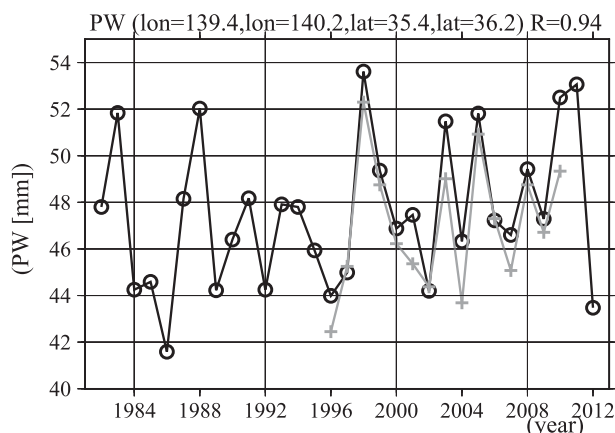


FIG. 6. Time series of the simulated precipitable water in August over REF Kanto and the 22-point averaged observed GPS precipitable water (Fig. 1b). The heavy black line with the open circles refers to the simulated values of precipitable water, and the gray line with plus signs is the observed values. The interannual correlation coefficient, mean bias, and root-mean-square error over the 15-yr period from 1996 to 2010 between observed and simulated values were 0.94, 1.17, and 1.55, respectively.

low-level southerlies are stronger over the Kanto District than over the Tokai District. Concurrent with these southerlies, relatively lower temperature air is transported from ocean to land.

c. Impact of SST on surface air temperature on an interannual time scale

The previous subsection showed that CTL was sufficiently realistic on an interannual time scale, as evaluated by the observational datasets. To understand the spatial pattern of the impact of SST over REF Kuroshio on the surface air temperature, we generated regression maps showing the interannual variation in the sensitivity of surface air temperature with area-averaged SST over REF Kuroshio (Fig. 8). The sensitivity of surface air temperature was defined by the difference in surface air temperature between the CTL and ClimSST experiments at each grid. Colors of regression coefficient were statistically significant.

Higher and statistically significant sensitivity was observed along the Pacific coastal region, particularly over the Kanto District. This indicates that the interannual variation in SST over REF Kuroshio can modulate surface air temperature along the Pacific coast. The sensitivities along the Sea of Japan coast were mostly statistically insignificant (Fig. 8), which indicates the sensitivities of surface air temperature along the Sea of Japan coast to SST over the REF Kuroshio were not systematic. This suggests that the impact of SST over the REF Kuroshio was small along the Sea of Japan coast.

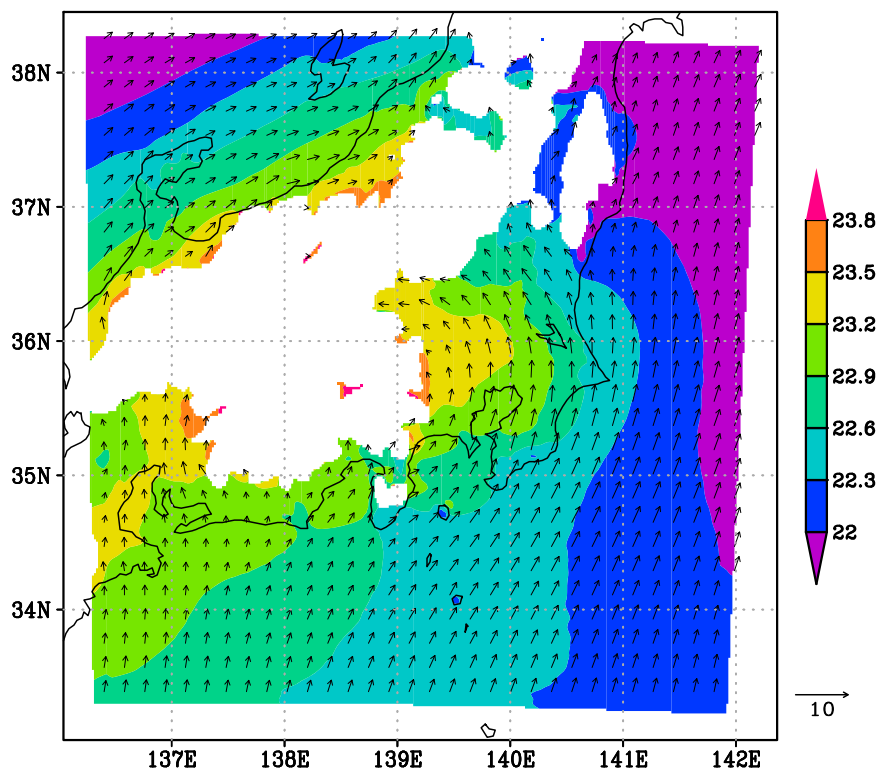


FIG. 7. Simulated climatological 950-hPa winds (m s^{-1}) and air temperature (K) in August over domain 2 for the 31-yr period from 1982 to 2012.

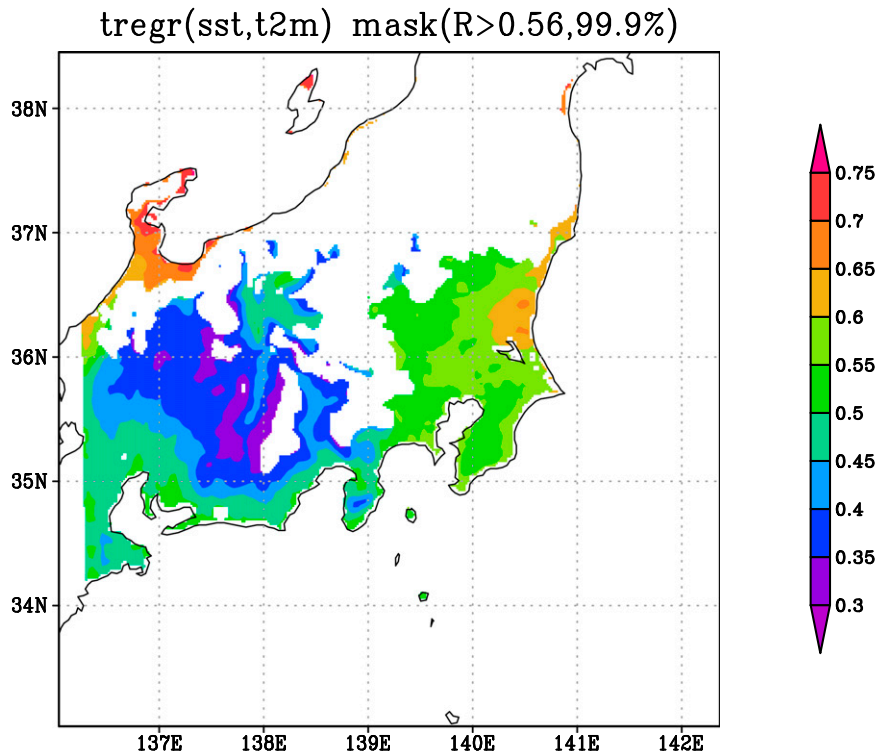


FIG. 8. Regression coefficient of the sensitivity of surface air temperature (K) in August to SST over REF Kuroshio on the normalized SST over REF Kuroshio during the 31-yr period from 1982 to 2012. All plotted values are statistically significant at the 99.9% level, as determined by correlation coefficients based on 29 degrees of freedom.

Additionally, to quantitatively examine the impact of SST on the surface air temperature over the Pacific side, we calculated the percentage variance in the simulated surface air temperature in the ClimSST experiments. The percentage variance was defined as the ratio of the total interannual variance in surface air temperature in ClimSST to that in CTL. Interannual variance in CTL was controlled primarily by atmospheric and oceanic impacts, whereas in ClimSST interannual variance was controlled primarily by atmospheric impact. Thus, the difference can be explained by the oceanic impact on the interannual variation in surface air temperature when we assume that the impacts can be divided linearly into atmospheric and oceanic impacts. In this paper, we assume that other impacts, such as land surface and nonlinear impacts, were unchanged because of SST changes.

The oceanic impact may be given quantitatively as

$$\text{Impact}_{\text{ocean}} = 1 - (\text{Vari}_{\text{climSST}} / \text{Vari}_{\text{CTL}}).$$

Here, $\text{Impact}_{\text{ocean}}$ is the impact of interannual variation in SST as a percentage, $\text{Vari}_{\text{climSST}}$ is the interannual variance of the monthly surface air temperature in the

ClimSST experiments, and Vari_{CTL} is the interannual variance of the monthly surface air temperature in the CTL experiments. The term $\text{Impact}_{\text{ocean}}$ is nondimensional.

The total variance in monthly mean surface air temperature over REF Kanto in CTL was 0.77 K^2 , whereas that in ClimSST was 0.53 K^2 (Fig. 9). Thus, the percentage variance was 0.688, indicating that 31.2% of the total variance in interannual variation in surface air temperature over REF Kanto was caused by interannual variation in SST over the calculation domains. In other words, when interannual variations in SST over the calculation domains were much smaller than the observed interannual variations in SST, the interannual variation in surface air temperature was reduced.

Figure 10 shows the spatial distribution of the oceanic impact. The oceanic impact was larger in the coastal regions than in the inland regions. Over the Kanto District, the oceanic impact was approximately 0.3. This result indicates that one-third of the interannual variation in surface air temperature was driven by the interannual variation in SST. Over the Tokai District, the oceanic impact was 0.4. The oceanic impact was larger over the Tokai District than the Kanto District because the total variance in surface air temperature over the

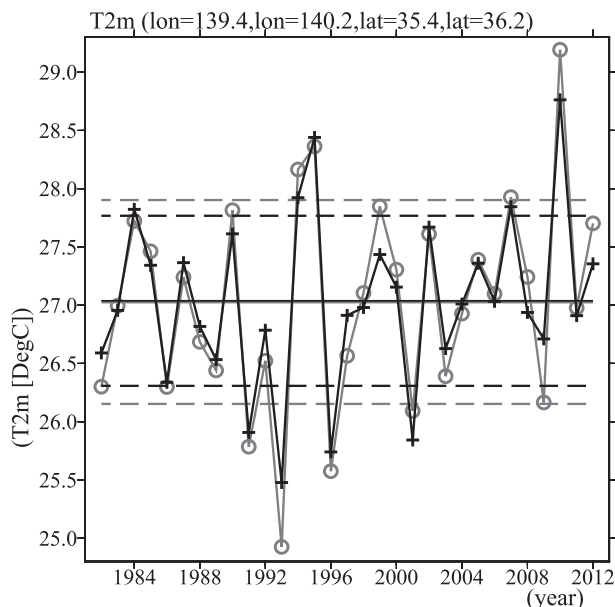


FIG. 9. Time series of the simulated surface air temperature in August over REF Kanto in the CTL (gray) and ClimSST (black) experiments. The climatological mean is shown as the black solid line. The gray (black) dashed lines show the $\pm 1\sigma$ (interannual standard deviation) from the climatological mean in the CTL (ClimSST) experiments.

Tokai District was smaller than that over the Kanto District (Fig. 11). Thus, the absolute oceanic impact over the Kanto District was slightly larger than that over the Tokai District.

d. Impact of SST over the Kuroshio region on surface air temperature over the Kanto District

Figure 12a shows the time series of SST anomalies over REF Kuroshio and the sensitivity of surface air temperature over REF Kanto. The sensitivity of surface air temperature was defined by the difference in surface air temperature over the Kanto District between the CTL and ClimSST experiments.

The warmer SST anomalies over the Kuroshio were associated with positive sensitivities in the surface air temperature over REF Kanto, whereas the colder anomalies corresponded to negative sensitivities. The correspondence between the SST anomalies and sensitivity in surface air temperature was clearer when the absolute SST anomaly values were larger. This result indicates that a warmer SST anomaly over the Kuroshio region induces warmer surface air temperature over the Kanto District.

Furthermore, it should be noted that the long-term change in SST over the Kuroshio was dominant. Concurrent with this long-term increase in SST, sensitivity of surface air temperature to SST has changed gradually

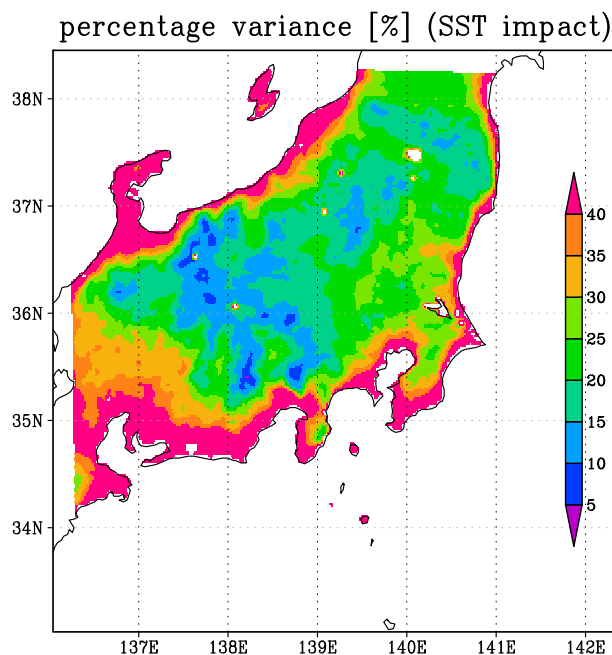


FIG. 10. Spatial distribution of oceanic impact shown as the percentage variance in monthly surface air temperature of ClimSST to that of CTL. The detailed formulation used to estimate oceanic impact is described in the text. The percentage variance is defined as the total interannual variance in surface air temperature in ClimSST to that in CTL.

from negative to positive since the middle of the 1990s (Fig. 12a). This result suggests that the increase in SST over the most recent three decades over the Kuroshio was responsible for a portion of the long-term increase in surface air temperature over the Pacific coastal region (see section 4d).

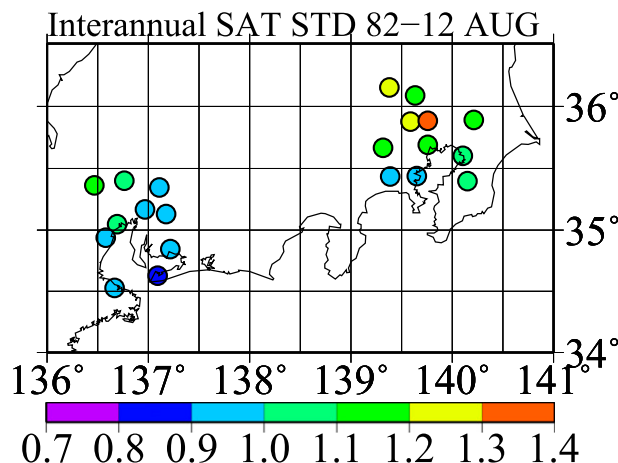


FIG. 11. Spatial distribution of observed interannual standard deviations in monthly surface air temperature (K) over the Kanto and Tokai Districts.

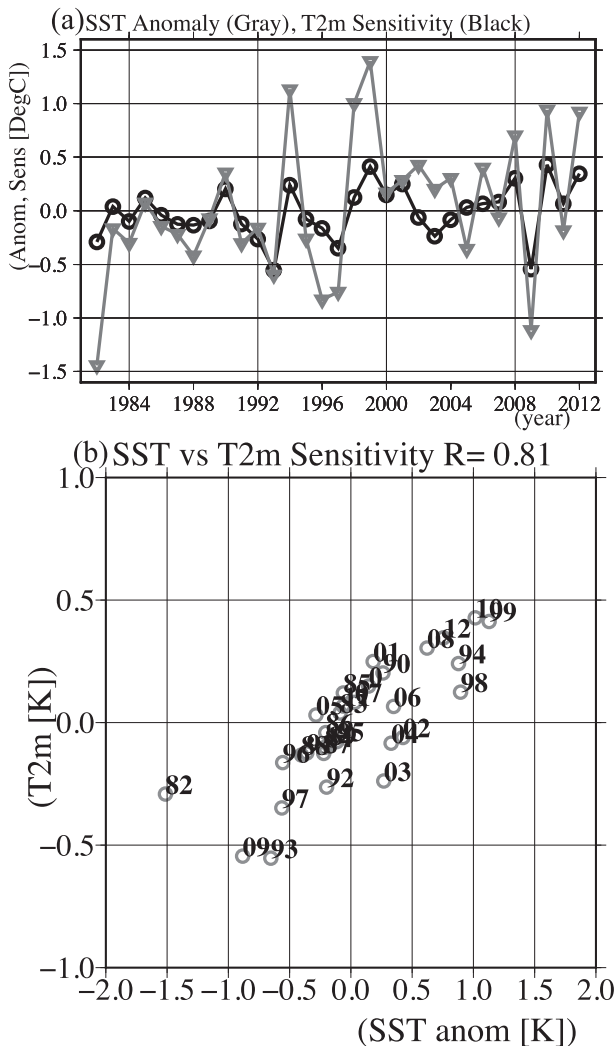


FIG. 12. (a) Time series of the SST sensitivity (black, open circles) of surface air temperature in August over REF Kanto and the SST anomaly (gray, open triangles) over REF Kuroshio during the 31-yr period from 1982 to 2012. (b) Scatterplot of the SST sensitivity of surface air temperature in August over REF Kanto and SST anomaly over REF Kuroshio with the same values used in (a). The sensitivity of surface air temperature to SST is defined as the difference in area-averaged surface air temperature over REF Kanto between the CTL and ClimSST experiments. The SST anomalies are averaged over REF Kuroshio.

e. Quantification of SST impact on surface air temperature

This subsection quantifies SST impact on the surface air temperature on an interannual time scale. Figure 12b shows a scatterplot between SST anomalies from the climatology over REF Kuroshio and sensitivities in surface air temperature over REF Kanto.

The sensitivity of surface air temperature clearly increased with the increase in SST over the Kuroshio

region. The relationship between surface air temperature and SST can be considered almost linear in the actual range of the interannual variation in SST over the Kuroshio region. Thus, higher SST over the Kuroshio region can induce higher surface air temperature over the Pacific coastal regions.

The calculated surface air temperature over REF Kanto increased by 0.41 K per 1-K SST warming over REF Kuroshio, based on a linear regression coefficient obtained by the method of least squares. Because the interannual standard deviation of SST over the Kuroshio region was approximately 0.6–0.8 K (Fig. 2), approximately 0.25–0.33 K of the interannual standard deviation in surface air temperature was attributable to the interannual variation in SST. Therefore, the impact of SST was considered quantitatively sufficient to account for the interannual variation in surface air temperature over the Pacific coast.

f. Diurnal variation in SST impact on surface air temperature

This subsection investigates the diurnal variation in the sensitivity of surface air temperature over the Kanto District to SST over the Kuroshio, because energy balance at the surface is much different during daytime and nighttime. Figure 13 shows the diurnal variation in the regression coefficient of the sensitivity of surface air temperature over REF Kanto against SST over REF Kuroshio and the correlation coefficient between the two as a function of Japan standard time (UTC +9h). Distinct diurnal variation in the sensitivity of surface air temperature was observed. During late afternoon and early morning, the sensitivity of surface air temperature was approximately 0.4–0.45 K per 1-K SST warming, whereas it was around 0.2 K per 1-K SST warming during daytime. This indicates that the sensitivity of surface air temperature over REF Kanto to SST over REF Kuroshio was considerably larger during nighttime.

4. Discussion

a. Horizontal temperature advection

The increase in surface air temperature could be attributable to horizontal temperature advection in the lower troposphere. Specifically, a warming signal indicates weakening of cold advection from sea to land. Figure 14 shows the regression coefficients for monthly mean 950-hPa winds and air temperature on the monthly mean SST anomaly in August over the key SST region for the 31 years from 1982 to 2012.

Regressed southerlies or southeasterlies were observed over the Pacific coastal region, indicating that

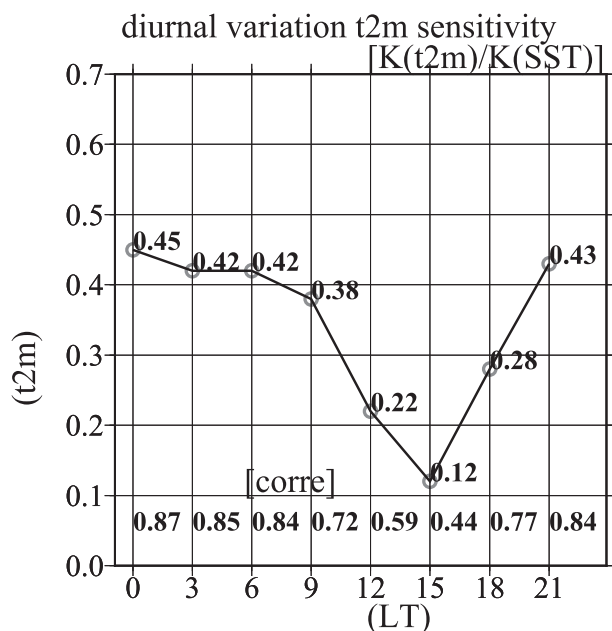


FIG. 13. Diurnal variation in the regression coefficient of the sensitivity of surface air temperature over REF Kanto against SST over REF Kuroshio and correlation coefficient between the two as a function of Japan standard time (JST; UTC + 9 h). Values with open circles are the regression coefficients at each local time. Values at the bottom of the panel show the correlation coefficients between the two as a function of local time. The sensitivity of surface air temperature to SST is defined as the difference in area-averaged surface air temperature over REF Kanto between the CTL and ClimSST experiments.

climatological low-level winds were enhanced. The enhanced southerlies can intensify climatological horizontal cold advection over the Kanto District. The climatological meridional wind speed was approximately 3 m s^{-1} . The enhanced meridional wind shown in the regression coefficient increased by approximately 10% of the total fields. Conversely, the meridional 950-hPa temperature gradient was reduced. The meridional 950-hPa air temperature gradient was weakened by approximately 10%. Therefore, the effect of the enhanced wind speed was canceled by the weakened meridional temperature gradient.

Figure 15 shows a scatter diagram between monthly mean SST values over REF Kuroshio and 950-hPa temperature advection heating over the Kanto District. The interannual variation in heating due to 950-hPa temperature advection over the Kanto region was positively correlated with SST anomalies over REF Kuroshio. However, the correlation was weak, explaining less than 20% of the total interannual variance in surface air temperature. Furthermore, the correlation was nearly 0 over REF Tokai. Therefore, we concluded that the effect of horizontal temperature advection is

not primary for the increase in surface air temperature over the Pacific coast.

The mechanism of change in low-level winds may be explained by the downward transport of momentum in the planetary boundary layer. Additionally, cyclonic anomalies associated with enhancement of the heat low over Honshu Island can intensify the low-level winds. However, it was not clear whether changes in local wind systems, such as sea and land breezes, were due to changes in the thermal horizontal gradient. Additionally, changes in the diurnal cycle of near-surface winds were not clear.

b. Sensitivity of surface energy balance to SST changes

To understand changes in the surface air temperature, we investigated the changes in surface energy balance derived from the law of energy conservation. Surface energy balance can be given by Eq. (2) of Zhang et al. (2011), originally from Wild et al. (2004). The sum of the absorbed shortwave and downward longwave radiation is defined as radiative input to the surface. The input is redistributed to upward longwave radiation (surface longwave emission), sensible and latent heat fluxes, and ground heat flux. We calculated net radiation R_n , defined as the sum of the sensible and latent heat fluxes, and ground heat flux.

We investigated the sensitivity of net radiation over the Kanto District to SST over REF Kuroshio (Fig. 16a). The results showed that changes in net radiation due to SST changes were almost random. The correlation coefficient between SST anomalies over the region south of the Pacific coast and net radiation at the surface over the Kanto District was 0.27. The interannual standard deviation of net radiation at the surface was 1.9 W m^{-2} . To understand why the sensitivity of the net radiation at the surface is unsystematic, we examined downward shortwave and longwave radiations at the surface.

The sensitivity of downward shortwave radiation at the surface to SST over REF Kuroshio was investigated, because the changes in surface albedo are negligible in this experiment. The results showed that changes in downward shortwave radiation due to SST changes were random because the correlation coefficient between SST anomalies over the southern region of the Pacific coast and downward shortwave radiation at the surface over the Kanto District was -0.05 (Fig. 16b), indicating negligible influence of SST interannual variability on cloud cover. Thus, the sensitivity of downward shortwave radiation at the surface to SST over REF Kuroshio was not systematic. In addition, the interannual standard deviation of

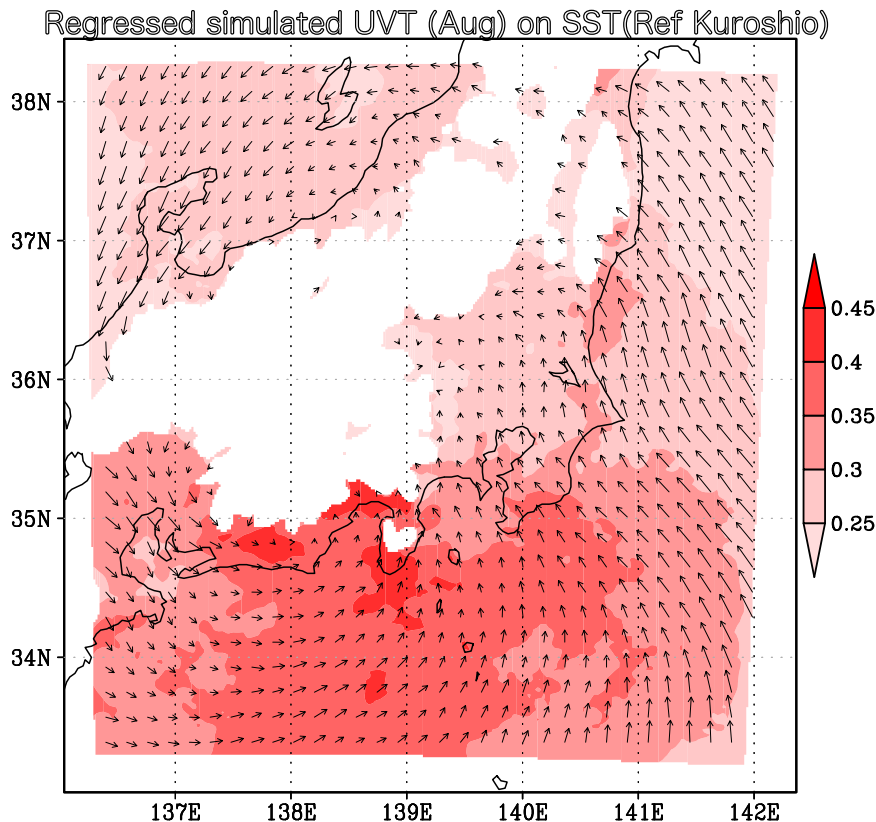


FIG. 14. Regressed simulated 950-hPa winds (m s^{-1}) and air temperature (K) in August on the normalized SST over REF Kuroshio during the 31-yr period from 1982 to 2012.

downward shortwave radiation at the surface was 3.2 W m^{-2} , which was comparable to that of net radiation at the surface. This implies that the unsystematic response of downward shortwave radiation at the surface contributed to the unsystematic response of net radiation at the surface.

Moreover, we examine the sensitivity of downward longwave radiation at the surface to SST over REF Kuroshio (Fig. 16c). The results showed clear sensitivity of downward longwave radiation at the surface over the Kanto District to SST over REF Kuroshio. A correlation coefficient between SST anomalies over the region south of the Pacific coast and downward longwave radiation at the surface over the Kanto District was 0.84. The increase in downward longwave radiation at the surface was approximately $2.3 \text{ W m}^{-2} (0.4 \text{ K})^{-1}$ of surface air temperature (Fig. 17b).

We simply calculated the increase in surface longwave emission due to surface air temperature warming in the vicinity of 300 K, which is almost the climatological mean. The maximum sensitivity of surface air temperature was 0.4 K in August 2010. From this estimation, the increase in upward longwave radiation was

approximately 2.4 W m^{-2} when the increase in surface air temperature was 0.4 K. Concurrent with the systematic sensitivity of downward longwave radiation at the surface over REF Kanto to SST over REF Kuroshio, the sensitivity of upward longwave radiation at the surface was also systematic, because the sensitivity of surface air temperature was systematic (Fig. 12b). It is noteworthy that the magnitudes of sensitivity of the downward and upward longwave radiations were comparable. In the following subsection, we discuss the mechanism of the increase in downward longwave radiation at the surface.

c. Physical mechanism of the increase in downward longwave radiation at the surface

As stated in the previous section, the increase in downward longwave radiation at the surface was approximately $2.3 \text{ W m}^{-2} (0.4 \text{ K})^{-1}$ of surface air temperature. The difference between CTL and ClimSST is only the prescribed SST condition. We examined the changes in surface heat fluxes over REF Kuroshio (Fig. 18). The increase in latent heat flux over ocean was considerably larger than that in sensible heat flux in this experiment,

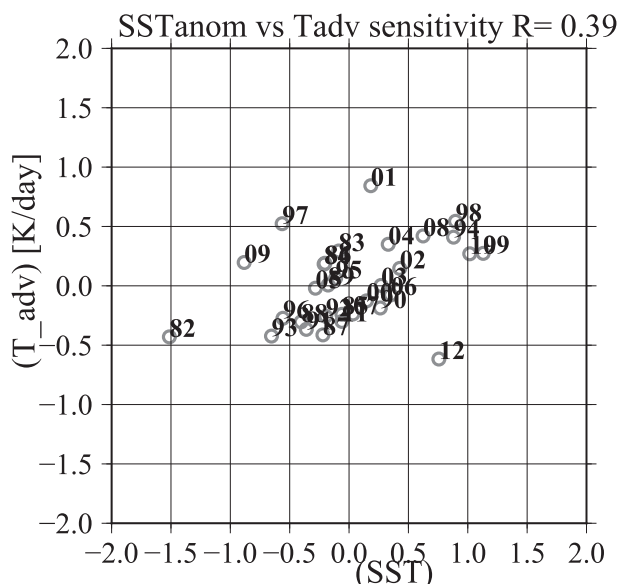


FIG. 15. Scatter diagram between the SST anomaly south of the Pacific coast of Japan (i.e., the Kuroshio region) and the SST sensitivity of 950-hPa thermal advective warming in August over REF Kanto. The sensitivity of 950-hPa thermal advective warming to SST is defined as the difference in area-averaged 950-hPa thermal advective warming over REF Kanto between the CTL and ClimSST experiments.

which resulted in an increase in water vapor (Fig. 19). This result can be explained by the temperature dependence of the Bowen ratio. Thus, the regional H_2O greenhouse gas warming due to the enhancement of water vapor supply from the ocean can be a candidate to explain the increase in downward longwave radiation

and surface air temperature, as direct heating by the sensible heat flux was very small.

Clear-sky downward longwave radiation at the surface can be roughly estimated by precipitable water and surface air temperature. Because changes in downward shortwave radiation were not correlated with changes in surface air temperature in our experiments, we assumed that the changes in cloud cover were random, as shown in Fig. 16b. Additionally, the effect of changes in cloud cover on downward longwave radiation at the surface can be smaller than those of precipitable water and surface air temperature under these moist conditions. Actually, the correlation between precipitable water or surface air temperature and all-sky downward longwave radiation at the surface from the estimation by a realistic regional climate model was very high (Fig. 17). Thus, we can use clear-sky downward longwave radiation at the surface here. We simply estimated the impact of changes in precipitable water and surface air temperature on clear-sky downward longwave radiation. A simple estimation using precipitable water and screen-level air temperature (1.5 m) was formulated by Allan et al. (2004). This formula was based on Prata (1996), who used water vapor pressure and screen-level air temperature. We used Eq. (1) from Allan et al. (2004), although we used air temperature at 2 m above the surface as the screen-level air temperature.

The simple estimation showed that clear-sky downward longwave radiation at the surface increased by approximately 2 W m^{-2} (2 mm^{-1}) of precipitable water when the total precipitable water was approximately 50 mm. Clear-sky downward longwave radiation at the

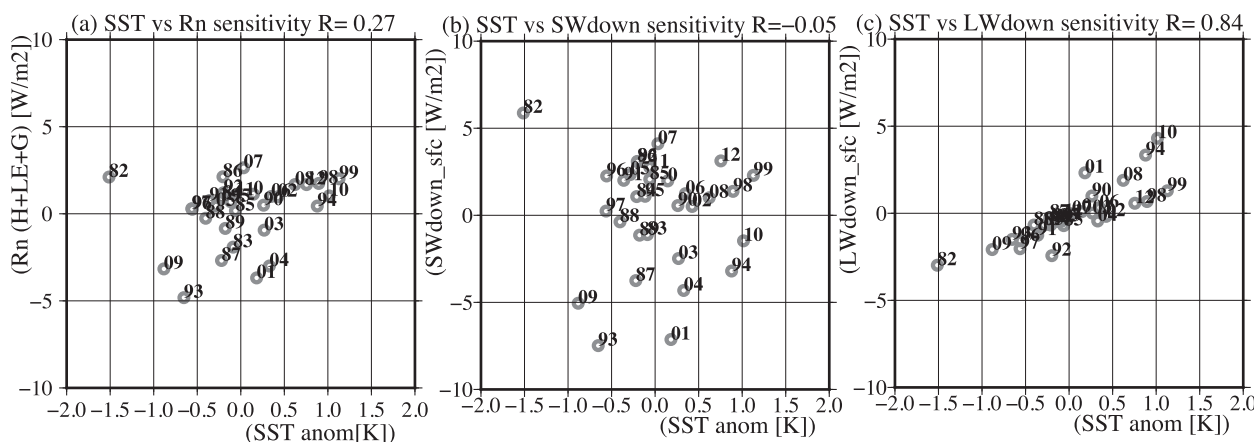


FIG. 16. (a) Scatter diagram between the sensitivities of net radiation at the surface over REF Kanto, which was calculated from the sum of the sensible, latent, and ground heat fluxes, to SST over REF Kuroshio. The sensitivity of net radiation at the surface to SST is defined as the difference in area-averaged net radiation at the surface over REF Kanto between the CTL and ClimSST experiments. (b) As in (a), but for downward shortwave radiation at the surface. (c) As in (a), but for downward longwave radiation at the surface. The values shown in the top right of each panel are interannual correlation coefficients.

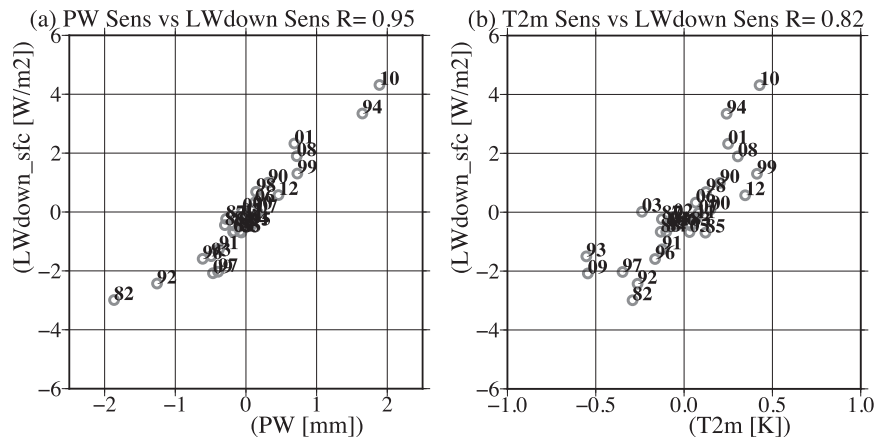


FIG. 17. (a) Scatter diagram between sensitivity in precipitable water over REF Kanto to SST over REF Kuroshio and that in downward longwave radiation at the surface over REF Kanto during the 31-yr period from 1982 to 2012. (b) As in (a), but for surface air temperature. The sensitivities in monthly mean precipitable water, downward longwave radiation at the surface, and surface air temperature to SST are defined as the differences between the CTL and ClimSST experiments.

surface increased by approximately 2 W m^{-2} (0.4 K) $^{-1}$ of surface air temperature at approximately 300 K. In the August 2010 case, precipitable water, surface air temperature, and downward longwave radiation at the surface increased by approximately 2 mm, 0.4 K, and 2.3 W m^{-2} , respectively, over the Kanto District. In addition, a larger increase in downward longwave radiation over the Kuroshio region south of the Kanto District was observed (not shown). Thus, the increase in longwave radiation due to precipitable water can be considered a quantitatively reasonable explanation for the increase in surface air temperature.

Furthermore, we also investigated the spatial distribution of the interannual variation in the sensitivity of precipitable water and vertically integrated water vapor fluxes with area-averaged SST over REF Kuroshio (Fig. 19). Again, the sensitivity of precipitable water and water vapor fluxes were defined by the differences between the CTL and ClimSST experiments. Higher sensitivity was observed over REF Kuroshio; the Kanto District; and the western area of the Kanto District, which was clearly explained by the enhanced evaporation and water vapor transports from the REF Kuroshio region. This spatial distribution was similar to that for

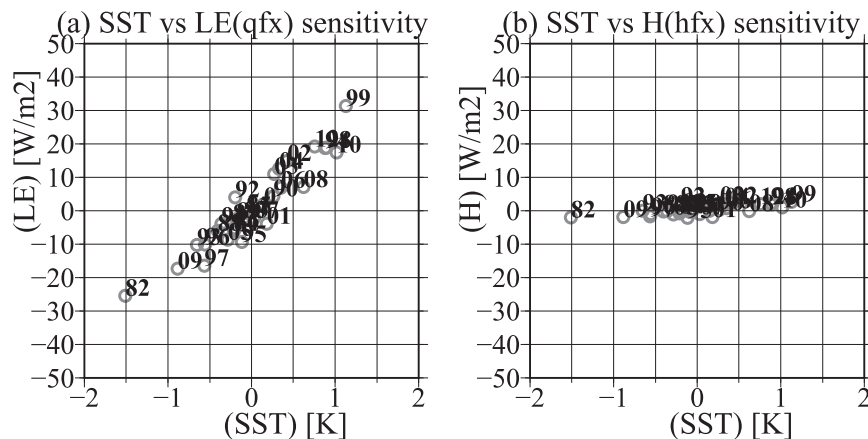


FIG. 18. (a) Scatter diagram between SST anomalies and sensitivity in latent heat flux at the sea surface over REF Kuroshio during the 31-yr period from 1982 to 2012. (b) As in (a), but for sensible heat flux. The sensitivities in latent and sensible heat fluxes to SST are defined as the differences between the CTL and ClimSST experiments.

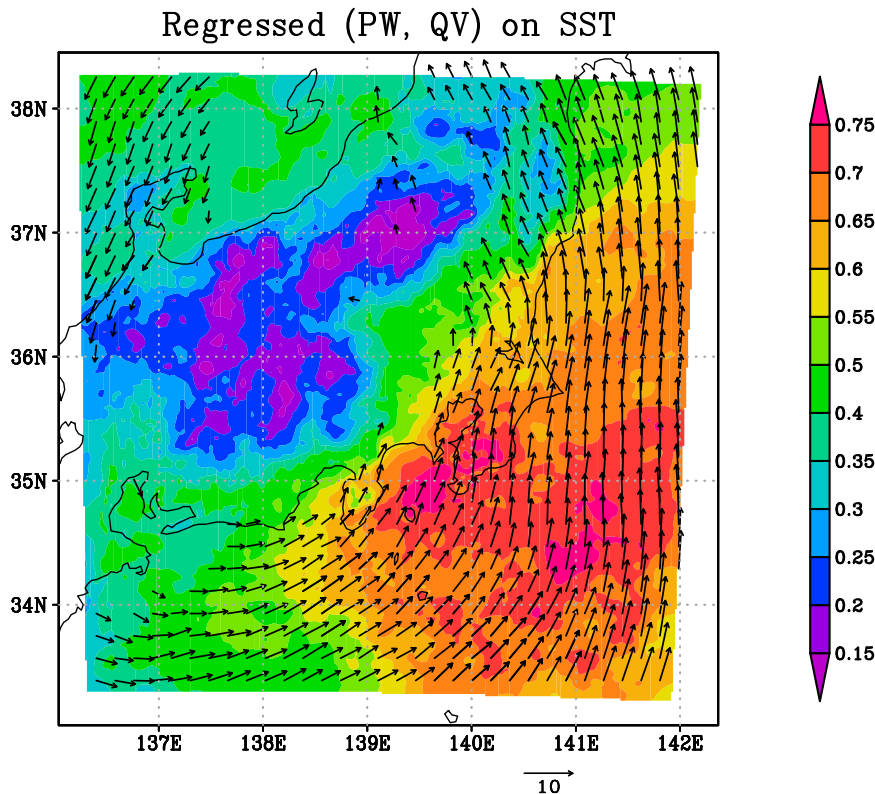


FIG. 19. Regression coefficient of the simulated precipitable water (mm) and vertically integrated water vapor fluxes ($\text{kg m}^{-1} \text{s}^{-1}$) in August on the normalized SST over REF Kuroshio during the 31-yr period from 1982 to 2012. All plotted vectors are statistically significant at the 99.9% level, as determined by correlation coefficients based on 29 degrees of freedom.

the sensitivity of surface air temperature to SST over REF Kuroshio (Fig. 8), supporting our proposed mechanism of regional H_2O greenhouse gas warming.

As mentioned above, the increases in surface air temperature, downward longwave radiation at the surface, and precipitable water are attributable to the increase in SST over the Kuroshio region south of the Kanto and Tokai Districts. When more water vapor is transported from the ocean to the land, the surface air temperature is warmed by H_2O greenhouse gas warming. Therefore, the high latent heat flux over the ocean caused by the increase in SST leads to increased water vapor transport from ocean to land, which results in warmer and wetter air masses over the Pacific coastal regions. In other words, regional H_2O greenhouse gas warming was enhanced.

The diurnal variation in the SST sensitivity of surface air temperature was much higher during nighttime (Fig. 13). This diurnal variation in the SST sensitivity of surface air temperature is also reasonably explained by our proposed mechanism of regional H_2O greenhouse gas warming, because changes in downward longwave radiation at the surface are the main modulators of

surface air temperature during the nighttime, whereas shortwave radiation is stronger than longwave radiation during the daytime.

d. Long-term changes in surface air temperature and SST

As shown in the previous sections, the impact of SST over the Kuroshio contributes one-third of the total interannual variance in surface air temperature on interannual time scales. Recently, Wu et al. (2012) showed that long-term increase in SST over the westerly boundary currents was 2 or 3 times larger than global mean SST warming. Although our estimation of the impact of SST over the Kuroshio on surface air temperature in the Pacific coastal regions may not be directly applicable to the long-term increase in SST impact on surface air temperature, it is likely that the enhanced long-term warming in SST over the Kuroshio significantly affects surface air temperature along the Pacific coastal region.

The estimated 31-yr long-term trends in surface air temperature over REF Kanto in the CTL and ClimSST experiments were 0.24 and $0.15 \text{ K (decade)}^{-1}$,

respectively. The estimated long-term trend in surface air temperature averaged from 11 monitoring points (Fig. 1) was $0.31 \text{ K (decade)}^{-1}$. This underestimation of the long-term trend in surface air temperature in the CTL experiments may be because of our experiments having constant CO_2 concentration. Nevertheless, the long-term trend of surface air temperature in ClimSST was much smaller than that in CTL. Approximately 30% of the long-term trend in surface air temperature over the Kanto District can be explained by the oceanic effect, although both long-term trends were not statistically significant, as evaluated by the nonparametric Mann–Kendall test. Additional studies on estimations of the oceanic impact of long-term trends and interdecadal variations in SST over the Kuroshio are required.

5. Conclusions

We applied a regional climate model to quantitatively estimate the impact of SST in and around the Kuroshio area on the climate of the Pacific coast region of Japan during 31 summers from 1982 to 2012. We performed CTL experiments driven by reanalysis and observational SST datasets. We conducted 31 one-month (August) sensitivity experiments (ClimSST) using climatological values for SSTs over a period of 31 years to examine the sensitivity of surface air temperature to SST. This value is robust, and it was estimated from many experiments under various atmospheric and oceanic conditions within the actual range of interannual variation in SST.

The results showed that the interannual variation in surface air temperature over the Pacific coast was simulated accurately in the CTL. The total interannual variance in surface air temperature over the Pacific coast in CTL was larger than that in ClimSST. The percentage variance in ClimSST to CTL was approximately 70%, which indicates that 30% of the interannual variance in surface air temperature was controlled by SST. If SST did not vary interannually, the interannual standard deviation for surface air temperature during August over the Kanto District would decrease from 0.88 to 0.73 K. Furthermore, it is noted that the long-term change in SST over the Kuroshio contributed in part to that in surface air temperature in the Pacific coastal region.

The impact of SST on surface air temperature can be estimated as a 0.4-K increase in daily mean surface air temperature over the Kanto region per 1-K increase in SST south of the Pacific coast; that is, over the Kuroshio region. Diurnal variation in the impact of SST was evident. The SST impact during nighttime was considerably greater than that during daytime, indicating that SST

exerts a marked effect on the minimum temperature in summer through the following mechanism.

The increase in surface air temperature over the Pacific coast induced by the increase in SST south of the Kanto District may be explained by the increased downward longwave radiation at the surface caused by the increase in precipitable water. It should be noted that the increase in air temperature by the advection term at 950 hPa was not highly correlated with the increase in surface air temperature. This suggests that the interannual variation in the horizontal temperature advection effect was not significant for the interannual variation in surface air temperature over the Pacific coastal region induced by SST warming over the upstream region of the low-level climatological southerly in summer. In other words, the interannual variation in surface air temperature can be affected by regional warming from H_2O greenhouse gas. This reasonably explains the diurnal variation in the SST sensitivity of surface air temperature.

Acknowledgments. We thank four anonymous referees for their constructive and valuable comments. The authors thank Mikiko Fujita and Kouichi Masuda for their valuable comments. This work was partly supported by the Global Environment Research Fund (2RF-1304) of the Ministry of the Environment (MOE); the start-up research fund of the Tokyo Metropolitan University; the Green Network of Excellence (GRENE) program; and the Research Program on Climate Change Adaptation (RECCA) Fund by the Ministry of Education, Culture, Sports, Science, and Technology (MEXT), Japan.

APPENDIX

Sensitivity of Surface Air Temperature over the Kanto District to SST Only South of the Kanto District

In this study, we showed the sensitivity of surface air temperature over the Kanto District to interannual SST variation over the whole calculation domain. This appendix estimates the quantitative sensitivity of the interannual variation in surface air temperature over the Kanto District to interannual SST variation in only the region south of the Kanto District.

To understand the impact of SST over only REF Kuroshio, we conducted a series of sensitivity experiments: that is, four 1-month experiments for August 2009–12. The SST anomalies averaged over REF Kuroshio are -0.9 , $+1.0$, 0.0 , and $+0.8$ in 2009, 2010, 2011, and 2012, respectively. Because of high computational

cost, the experiments were less extensive than the main experiments. The numerical design of these experiments was the same as that of CTL, except that SST over the whole domain outside of REF Kuroshio was replaced by the climatology from 1982 to 2012. Thus, SST over only REF Kuroshio varied interannually. These sensitivity experiments are referred to as KuroshioSST. Because the area of interannual SST variation in KuroshioSST was much smaller than that in CTL, the sensitivity in KuroshioSST may be much smaller than that in CTL. Or the sensitivity in KuroshioSST may be largely different from that in CTL if the SST over the Sea of Japan or Pacific Ocean west of Japan has a significant impact on surface air temperature over the Kanto District.

The results showed that the sensitivity of surface air temperature over the Kanto District was basically contributed by the SST over the REF Kuroshio region. The sign of the sensitivity between KuroshioSST and ClimSST was similar to that between CTL and ClimSST. The magnitude of the sensitivity to SST over REF Kuroshio in KuroshioSST was approximately 50% in 2010 and 40% in 2012 of that in CTL in years of positive SST anomaly over REF Kuroshio, whereas it was approximately 30% in 2009 in a year of negative SST anomaly over REF Kuroshio. This weaker sensitivity in the year of negative SST anomaly can be explained by differences in atmospheric circulation between positive SST and negative SST years. In general, the negative SST anomaly over the Kuroshio corresponded to cold years over Japan that was caused by a weaker westward expansion of the subtropical high. Climatological southerlies along the periphery of the subtropical high (Fig. 7) were weaker or sometimes became northerly. Thus, interannual SST variation over the Pacific Ocean west of Japan may be important for the interannual variation in surface air temperature in cold years over the Kanto district. In addition, the SST sensitivity of surface air temperature over the Kanto district in a normal SST year (2011) was very small in both SSTKuroshio and CTL experiments.

This appendix indicates that the key region of oceanic impact on the surface air temperature over the Kanto District is mainly over REF Kuroshio.

REFERENCES

- Allan, R. P., M. A. Ringer, J. A. Pamment, and A. Slingo, 2004: Simulation of the Earth's radiation budget by the European Centre for Medium-Range Weather Forecasts 40-year reanalysis (ERA40). *J. Geophys. Res.*, **109**, D18107, doi:[10.1029/2004JD004816](https://doi.org/10.1029/2004JD004816).
- Berrisford, P., D. Dee, K. Fielding, M. Fuentes, P. Kallberg, S. Kobayashi, and S. Uppala, 2009: The ERA-Interim Archive, version 1.0. ECMWF Tech Rep. ERA report series 1, 16 pp.
- Chen, F., and J. Dudhia, 2001: Coupling an advanced land surface–hydrology model with the Penn State–NCAR MM5 modeling system. Part I: Model implementation and sensitivity. *Mon. Wea. Rev.*, **129**, 569–585, doi:[10.1175/1520-0493\(2001\)129<0569:CAALSH>2.0.CO;2](https://doi.org/10.1175/1520-0493(2001)129<0569:CAALSH>2.0.CO;2).
- Enomoto, T., B. J. Hoskins, and Y. Matsuda, 2003: The formation mechanism of the Bonin high in August. *Quart. J. Roy. Meteor. Soc.*, **129**, 157–178, doi:[10.1256/qj.01.211](https://doi.org/10.1256/qj.01.211).
- Fujita, M., A. Wada, T. Iwabuchi, and C. Rocken, 2012: GPS precipitable water vapor dataset for climate science. *Proc. Int. Technical Meeting of the Satellite Division of the Institute of Navigation (ION GNSS 2012)*, Nashville, TN, Institute of Navigation, 3454–3458.
- Hong, S., and J. Lim, 2006: The WRF single-moment 6-class microphysics scheme (WSM6). *J. Korean Meteor. Soc.*, **42**, 129–151.
- Iacono, M. J., J. S. Delamere, E. J. Mlawer, M. W. Shephard, S. A. Clough, and W. D. Collins, 2008: Radiative forcing by long-lived greenhouse gases: Calculations with the AER radiative transfer models. *J. Geophys. Res.*, **113**, D13103, doi:[10.1029/2008JD009944](https://doi.org/10.1029/2008JD009944).
- Janjić, Z. I., 1994: The step-mountain eta coordinate model: Further developments of the convection, viscous sublayer, and turbulence closure schemes. *Mon. Wea. Rev.*, **122**, 927–945, doi:[10.1175/1520-0493\(1994\)122<0927:TSMECM>2.0.CO;2](https://doi.org/10.1175/1520-0493(1994)122<0927:TSMECM>2.0.CO;2).
- Kobayashi, S., and Coauthors, 2015: The JRA-55 Reanalysis: General specifications and basic characteristics. *J. Meteor. Soc. Japan*, **93**, 5–48, doi:[10.2151/jmsj.2015-001](https://doi.org/10.2151/jmsj.2015-001).
- Kosaka, Y., and H. Nakamura, 2006: Structure and dynamics of the summertime Pacific–Japan teleconnection pattern. *Quart. J. Roy. Meteor. Soc.*, **132**, 2009–2030, doi:[10.1256/qj.05.204](https://doi.org/10.1256/qj.05.204).
- Koseki, S., and M. Watanabe, 2010: Atmospheric boundary layer response to mesoscale SST anomalies in the Kuroshio Extension. *J. Climate*, **23**, 2492–2507, doi:[10.1175/2009JCLI2915.1](https://doi.org/10.1175/2009JCLI2915.1).
- Lindzen, R. S., and S. Nigam, 1987: On the role of sea surface temperature gradients in forcing low-level winds and convergence in the tropics. *J. Atmos. Sci.*, **44**, 2418–2436, doi:[10.1175/1520-0469\(1987\)044<2418:OTROSS>2.0.CO;2](https://doi.org/10.1175/1520-0469(1987)044<2418:OTROSS>2.0.CO;2).
- Minobe, S., A. Kuwano-Yoshida, N. Komori, S.-P. Xie, and R. J. Small, 2008: Influence of the Gulf Stream on the troposphere. *Nature*, **452**, 206–209, doi:[10.1038/nature06690](https://doi.org/10.1038/nature06690).
- , M. Miyashita, A. Kuwano-Yoshida, H. Tokinaga, and S.-P. Xie, 2010: Atmospheric response to the Gulf Stream: Seasonal variations. *J. Climate*, **23**, 3699–3719, doi:[10.1175/2010JCLI3359.1](https://doi.org/10.1175/2010JCLI3359.1).
- Nitta, T., 1987: Convective activities in the tropical western Pacific and their impact on the Northern Hemisphere summer circulation. *J. Meteor. Soc. Japan*, **65**, 373–390.
- Peng, S., W. A. Robinson, and M. P. Hoerling, 1997: The modeled atmospheric response to midlatitude SST anomalies and its dependence on background circulation states. *J. Climate*, **10**, 971–987, doi:[10.1175/1520-0442\(1997\)010<0971:TMARTM>2.0.CO;2](https://doi.org/10.1175/1520-0442(1997)010<0971:TMARTM>2.0.CO;2).
- Prata, A., 1996: A new long-wave formula for estimating downward clear-sky radiation at the surface. *Quart. J. Roy. Meteor. Soc.*, **122**, 1127–1151, doi:[10.1002/qj.49712253306](https://doi.org/10.1002/qj.49712253306).
- Reynolds, R., N. Rayner, T. Smith, D. Stokes, and W. Wang, 2002: An improved in situ and satellite SST analysis for climate.

- J. Climate*, **15**, 1609–1625, doi:[10.1175/1520-0442\(2002\)015<1609:AIISAS>2.0.CO;2](https://doi.org/10.1175/1520-0442(2002)015<1609:AIISAS>2.0.CO;2).
- Skamarock, W. C., and Coauthors, 2008: A description of the Advanced Research WRF version 3. NCAR Tech. Note NCAR/TN475+STR, 113 pp., doi:[10.5065/D68S4MVH](https://doi.org/10.5065/D68S4MVH).
- Wallace, J. M., T. Mitchell, and C. Deser, 1989: The influence of sea-surface temperature on surface wind in the eastern equatorial Pacific: Seasonal and interannual variability. *J. Climate*, **2**, 1492–1499, doi:[10.1175/1520-0442\(1989\)002<1492:TOSST>2.0.CO;2](https://doi.org/10.1175/1520-0442(1989)002<1492:TOSST>2.0.CO;2).
- Wild, M., A. Ohmura, H. Gilgen, and D. Rosenfeld, 2004: On the consistency of trends in radiation and temperature records and implications for the global hydrological cycle. *Geophys. Res. Lett.*, **31**, L11201, doi:[10.1029/2003GL019188](https://doi.org/10.1029/2003GL019188).
- Wu, L., and Coauthors, 2012: Enhanced warming over the global subtropical western boundary currents. *Nat. Climate Change*, **2**, 161–166, doi:[10.1038/nclimate1353](https://doi.org/10.1038/nclimate1353).
- Xu, H., H. Tokinaga, and S.-P. Xie, 2010: Atmospheric effects of the Kuroshio large meander during 2004–05. *J. Climate*, **23**, 4704–4715, doi:[10.1175/2010JCLI3267.1](https://doi.org/10.1175/2010JCLI3267.1).
- Zhang, T., M. P. Hoerling, J. Perlwitz, D.-Z. Sun, and D. Murray, 2011: Physics of U.S. surface temperature response to ENSO. *J. Climate*, **24**, 4874–4887, doi:[10.1175/2011JCLI3944.1](https://doi.org/10.1175/2011JCLI3944.1).